

# The Conservation of Helicity in Hurricane Andrew (1992) and the Formation of the Spiral Rainband

XU Yamei<sup>\*1,2</sup> (徐亚梅) and WU Rongsheng<sup>1</sup> (伍荣生)

<sup>1</sup>*Department of Atmosphere Science, Nanjing University, Nanjing 210093*

*Key Laboratory of Mesoscale Severe Weather of Ministry of Education, China*

<sup>2</sup>*Department of Geoscience, Zhejiang University, Hangzhou 310028*

(Received 3 November 2002; revised 3 September 2003)

## ABSTRACT

The characteristics of helicity in a hurricane are presented by calculating the MM5 model output in addition to theoretical analysis. It is found that helicity in a hurricane mainly depends on its horizontal component, whose magnitude is about 100 to 1000 times larger than its vertical component. It is also found that helicity is approximately conserved in the hurricane. Since the fluid has the intention to adjust the wind shear to satisfy the conservation of helicity, the horizontal vorticity is even larger than the vertical vorticity, and the three-dimensional vortices slant to the horizontal plane except in the inner eye. There are significant horizontal vortices and inhomogeneous helical flows in the hurricane. The formation of the spiral rainband is discussed by using the law of horizontal helical flows. It is closely related to the horizontal strong vortices and inhomogeneous helical flows.

**Key words:** helicity, conservation, helical flow, spiral rainband

## 1. Introduction

Helicity, which is defined as the volume integral of the inner vector product of vorticity and velocity, has been intriguing and perplexing fluid dynamicists for a number of years. Pseudoscalar ‘helicity’ can be associated with the topological properties of the field lines. The magnetic helicity is constant for the motion in ideal magnetohydrodynamics (Elsasser, 1956), as the field lines are frozen into the fluid as it moves. Similarly, the fluid helicity is constant for the motion in ideal hydrodynamics when all external forces are due to potentials (Maffat, 1969, 1978, 1981). Meteorologists are more interested in its property of atmospheric flows. Helicity has been found in several types of atmospheric flows, like turning shear flows (Ekman-layer, baroclinic-layer), boundary layer vortices, or rotating thunderstorms. A number of studies have paid attention to its conservation. Eting (1985) showed that the helicity is an invariant property of inviscid incompressible flow. Wu and Tan (1989), and Tan and Wu (1994) discussed the conservation of helicity as a generalized vorticity. Helicity is conserved in inviscid atmospheric flow when geostrophic balance and static equilibrium are satisfied. Many other works have been more inter-

ested in helicity affecting the cascade process in developed turbulence (Maffat, 1981). Helical flows are more stable than non-helical flows due to the suppression of nonlinear interaction. The intense supercell thunderstorms tend to be strongly helical and develop in an environment with a helical wind field (Lilly, 1986). High helicity can suppress turbulent dissipation. The helicity of long-lived storms is dominant. Lilly (1990) supposed the effect of helicity on direct generation of tornadic vortices may be important.

Although a number of studies have provided valuable insight into helical flows in the atmosphere, most of them placed their attention on perfect fluids such as barotropic inviscid and incompressible flows. We are concerned with typhoons and feel that helicity can play an important role in typhoon research work. Since we have not found any research work on helicity in typhoons, it is interesting to study its scale and time variant properties as well as the relation of helicity with cloud and rain. The results will help to simplify the complex equations and discover physical processes, which are still ambiguous.

In the next section, we present formulas that may be used in the following sections and theoretically show

\*E-mail: xym666@263.net Current affiliation: Department of Geoscience, Zhejiang University, Hangzhou 310028.

the variation of helicity in a real viscid and compressible atmosphere. By calculating the model output of hurricane Andrew (1992), the general features of helicity are presented in section 3. In section 4, the time invariant characteristic of helicity in hurricanes is studied and the conservation is used to explain the formation of significant horizontal vortices and inhomogeneous helical flows. The formation of spiral rainbands is discussed by using the rule of horizontal helical flows in section 5. Conclusions are given in section 6.

## 2. The conservation of helicity in the atmosphere

Helicity density, which is the dot product of velocity and vorticity, is defined as

$$h = \mathbf{V} \cdot \nabla \times \mathbf{V}. \quad (1)$$

For convenience, we also define  $h_x, h_y$ , and  $h_z$  as the product of velocity and vorticity in  $x, y$ , and  $z$  directions. The three components of helicity density in local rectangular coordinates are

$$\begin{cases} h_x = u \left( \frac{\partial w}{\partial y} - \frac{\partial v}{\partial z} \right), \\ h_y = v \left( \frac{\partial u}{\partial z} - \frac{\partial w}{\partial x} \right), \\ h_z = w \left( \frac{\partial v}{\partial x} - \frac{\partial u}{\partial y} \right). \end{cases} \quad (1')$$

Similarly, in cylindrical coordinates  $(r, \theta, z)$ , the horizontal components of the helicity density in the radial and tangential directions  $h_r$  and  $h_t$  can be expressed as

$$\begin{cases} h_r = V_r \left( \frac{1}{r} \frac{\partial w}{\partial \theta} - \frac{\partial V_t}{\partial z} \right), \\ h_t = V_t \left( \frac{\partial V_r}{\partial z} - \frac{\partial w}{\partial r} \right). \end{cases} \quad (1'')$$

Total helicity  $H$  is defined as

$$H = \iiint h d\tau. \quad (2)$$

We start with the primitive equations of three-dimensional viscid motion to obtain the time variant equations of helicity. The momentum equation is expressed as

$$\frac{\partial \mathbf{V}}{\partial t} + (\mathbf{V} \cdot \nabla) \mathbf{V} = \mathbf{T} - 2\boldsymbol{\Omega} \times \mathbf{V}, \quad (3)$$

where

$$\mathbf{T} = -\frac{1}{\rho} \nabla p + \mathbf{g} + \mathbf{F}$$

and  $\mathbf{F}$  is the frictional stress. Taking the curl of (3), we obtain the vorticity equation as

$$\frac{\partial \boldsymbol{\xi}}{\partial t} - \nabla \times (\mathbf{V} \times \boldsymbol{\xi}_a) = \nabla \times \mathbf{T}, \quad (4)$$

where

$$\boldsymbol{\xi}_a = \boldsymbol{\xi} + 2\boldsymbol{\Omega} = \nabla \times \mathbf{V} + 2\boldsymbol{\Omega}$$

is absolute vorticity and  $\boldsymbol{\xi}$  is relative vorticity.

By summing the vector product of Eq. (3) with  $\boldsymbol{\xi}$  and of Eq. (4) with  $\mathbf{V}$ , we obtain the helicity equation of three-dimensional viscid motion,

$$\begin{aligned} \frac{\partial (\mathbf{V} \cdot \boldsymbol{\xi})}{\partial t} + \nabla \cdot \left[ \mathbf{V} \times \nabla \left( \frac{\mathbf{V}^2}{2} \right) - \mathbf{V} \times \boldsymbol{\xi}_a \times \mathbf{V} - \mathbf{T} \times \mathbf{V} \right] \\ = 2(\nabla \times \mathbf{V}) \cdot (\mathbf{T} - 2\boldsymbol{\Omega} \times \mathbf{V}). \end{aligned} \quad (5)$$

Equation (5) is then rewritten as

$$\frac{\partial h}{\partial t} + \nabla \cdot \mathbf{M} = 2(\nabla \times \mathbf{V}) \cdot (\mathbf{T} - 2\boldsymbol{\Omega} \times \mathbf{V}), \quad (5')$$

where

$$\mathbf{M} = \mathbf{V} \times \nabla \left( \frac{\mathbf{V}^2}{2} \right) - \mathbf{V} \times \boldsymbol{\xi}_a \times \mathbf{V} - \mathbf{T} \times \mathbf{V}.$$

Adding term  $(\mathbf{V} \cdot \nabla)h$  to each side of Eq. (5'), gives

$$\frac{dh}{dt} + \nabla \cdot \mathbf{M} = 2(\nabla \times \mathbf{V}) \cdot (\mathbf{T} - 2\boldsymbol{\Omega} \times \mathbf{V}) + (\mathbf{V} \cdot \nabla)h. \quad (6)$$

The second term on the right-hand side of (6) can be recast in the form of

$$(\mathbf{V} \cdot \nabla)h = \nabla \cdot (h\mathbf{V}) - h\nabla \cdot \mathbf{V}.$$

Then Eq. (6) can be rewritten as

$$\frac{dh}{dt} + \nabla \cdot \mathbf{M}' = 2(\nabla \times \mathbf{V}) \cdot (\mathbf{T} - 2\boldsymbol{\Omega} \times \mathbf{V}) - h\nabla \cdot \mathbf{V}, \quad (6')$$

where

$$\begin{aligned} \mathbf{M}' &= \mathbf{M} - h\mathbf{V} \\ &= \mathbf{V} \times \left[ \nabla \left( \frac{\mathbf{V}^2}{2} \right) - \boldsymbol{\xi}_a \times \mathbf{V} + \mathbf{T} \right] - h\mathbf{V}. \end{aligned}$$

The integral of  $\nabla \cdot \mathbf{M}'$  in a whole enclosed atmosphere as well as in an isolated system with little flux across boundaries, such as a typhoon, is equal to zero.

Since

$$\begin{aligned} \frac{dH}{dt} &= \frac{d}{dt} \iiint h d\tau \\ &= \iiint \frac{dh}{dt} d\tau + \iiint h \nabla \cdot \mathbf{V} d\tau, \end{aligned}$$

the following result is obtained by integrating Eq. (6') with respect to the whole volume,

$$\begin{aligned} \frac{dH}{dt} &= \iiint 2(\nabla \times \mathbf{V}) \cdot (\mathbf{T} - 2\boldsymbol{\Omega} \times \mathbf{V}) d\tau \\ &= 2 \iiint \sigma d\tau, \end{aligned} \quad (7)$$

where

$$\begin{aligned} \sigma &= (\nabla \times \mathbf{V}) \cdot (\mathbf{T} - 2\boldsymbol{\Omega} \times \mathbf{V}) \\ &= (\nabla \times \mathbf{V}) \cdot \left( -\frac{1}{\rho} \nabla p + \mathbf{g} + \mathbf{F} - 2\boldsymbol{\Omega} \times \mathbf{V} \right). \end{aligned}$$

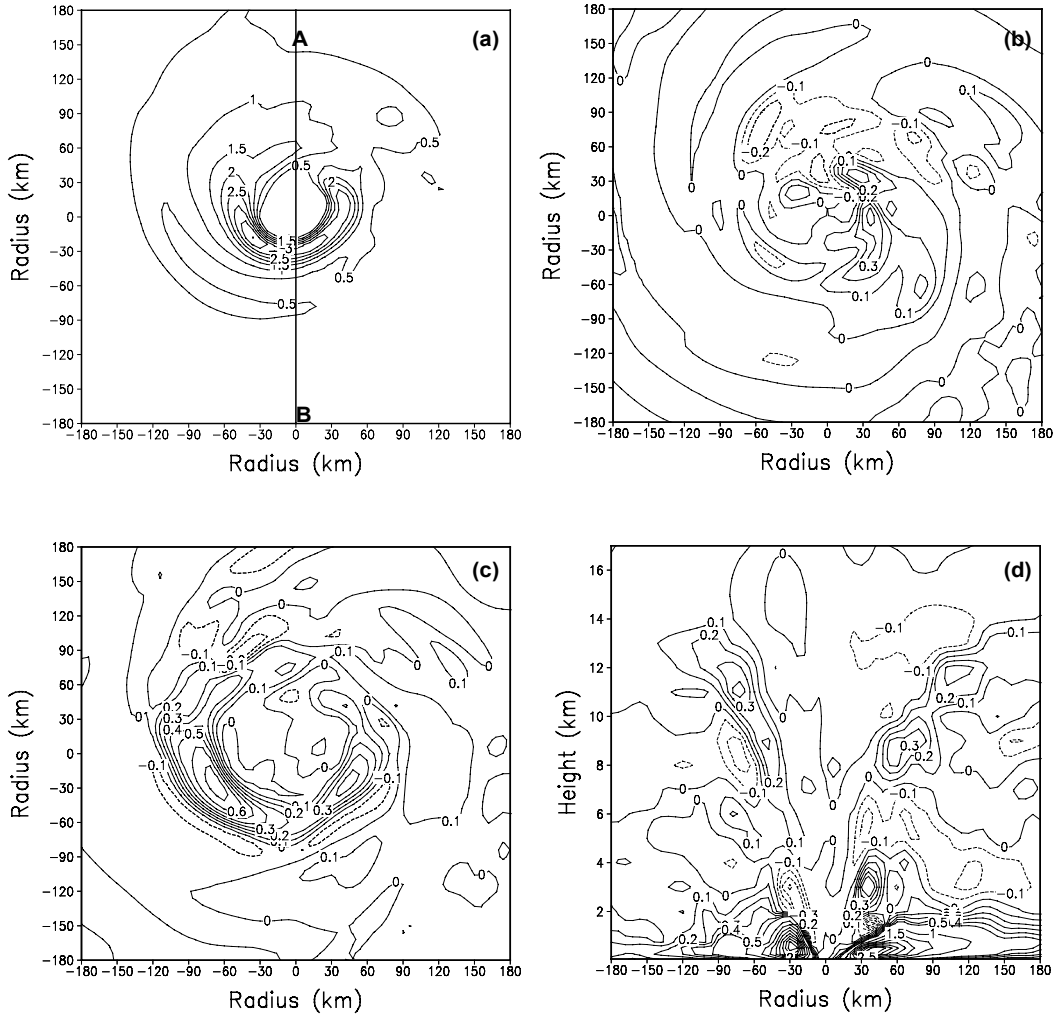


**Fig. 1.** Helicity density ( $h$ ,  $\text{m s}^{-2}$ ) of hurricane Andrew at 2100 UTC 23 August 1992. Radius is the distance from the center of the hurricane. (a) at 1 km; (b) at 5 km; (c) at 10 km; (d) vertical cross section along line AB in panel a.

Thus, the time variant property of the total helicity is dependent on the volume integral of  $\sigma$ . If  $\sigma$  equals zero or  $\iiint \sigma d\tau$  is zero, total helicity is conserved. For convenience, we define  $b$  as the vertical net force and  $\mathbf{D}$  as the horizontal net force. We also define  $\xi_s$  and  $\zeta$  as the horizontal vorticity and vertical vorticity respectively. Equation (7) is then simplified as

$$\frac{dH}{dt} = 2 \iiint (\xi_s \cdot \mathbf{D} + \zeta b) d\tau. \quad (8)$$

### 3. General features of helicity and significant horizontal vortices

In this section, the general features of helicity are presented.

First of all, the scale and sign of  $h$  (defined by formula (1)) are investigated. Since vertical vorticity

is more significant than horizontal vorticity for large scale motion, the vertical component of helicity represents the scale of the helicity. In a hurricane, the scale of vertical velocity is about  $O(1 \text{ m s}^{-1})$  and vertical vorticity is about  $O(0.5 \times 10^{-3} \text{ s}^{-1})$  (Liu et al., 1997). If its vertical eddy is significant, the scale of  $h$  is  $O(10^{-3} \text{ m s}^{-2})$ . Both vertical velocity and vorticity are positive in a cyclone and negative in an anticyclone.  $h$  is positive in both cyclones and anticyclones (Wu, 2002). It is reasonable to deduce that  $h$  is positive except in the inner eye, which is suggested to be the only exception for its downdraft and positive vertical vorticity. The theoretical conclusions must be verified by the observational facts.

The greatest difficulty in hurricane research is the lack of high-resolution observational data. The best

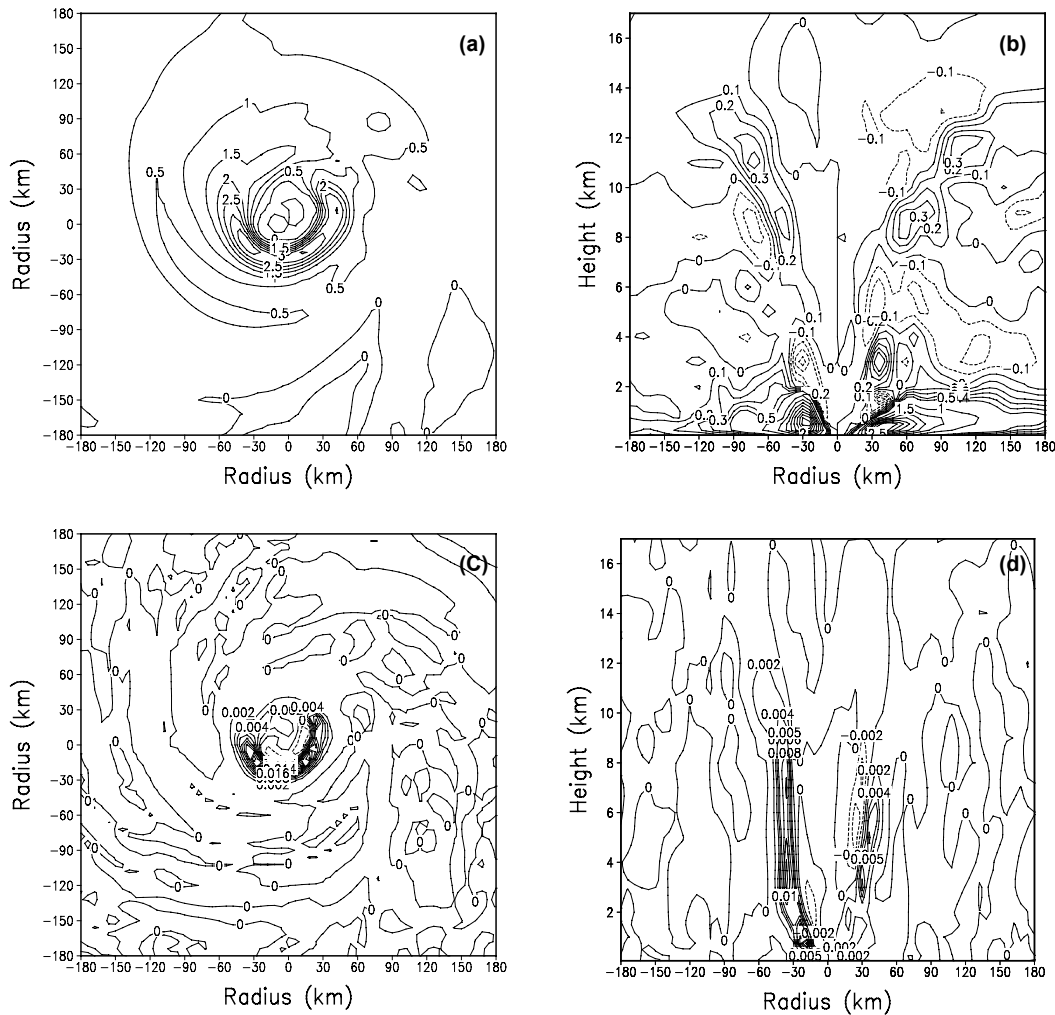


**Fig. 2.** Horizontal and vertical components of helicity density calculated by formula (1''). (a) horizontal component ( $h_r + h_t$ ) at 1 km; (b) the same as Fig. 1 (d) but for  $h_r + h_t$ ; (c) vertical component  $h_z$  at 1 km; (d) the same as Fig. 1d but for  $h_z$ .

way may be to analyze successive model output data to discuss the features of a hurricane. Andrew is a hurricane that was the most serious disaster in the history of the United States. Its simulation has been made and verified by Liu et al. (1997). The model system is the PSU-NCAR nonhydrostatic, two-way interactive, movable, triply-nested grid, 3D mesoscale model (MM5, version 2). The model physics include Blackadar PBL parameterization and a cloud-radiation interaction scheme. The model water cycles include the simultaneous use of the Betts-Miller deep and shallow convective parameterization and the Tao-Simpson cloud microphysics scheme for the 54-km and 18-km grid meshes, but only the latter is used for the 6-km grid mesh. In this study, the model output of the finest mesh domain with a grid size of 6-km is used.

Equation (1) is used to calculate  $h$  of Andrew at

the mature stage (at 2100 UTC 23 August 1992). The calculated values are shown in Fig. 1. Figures 1a, b, and c are the distribution of  $h$  at low (1 km), middle (5 km), and high (10 km) levels respectively. Figure 1d is the vertical cross section along line AB in Fig. 1a. The result is interesting. First,  $h$  is much larger than  $10^{-3} \text{ m s}^{-2}$ . Its order is about  $O(1 \text{ m s}^{-2})$  in the planetary boundary layer and  $O(0.1 \text{ m s}^{-2})$  in the layers above the boundary layer. Second, except in the planetary boundary layer,  $h$  is negative in the eyewall and spiral band as well as in the inner eye. Thirdly, the inhomogeneous feature is significant.

In order to clarify the above characteristics, the horizontal and vertical components of helicity are calculated separately by using Eqs. (1') and (1''). Figures 2 and 3 present some of the calculated values. Figures 2a and 2b show the horizontal component of helicity.

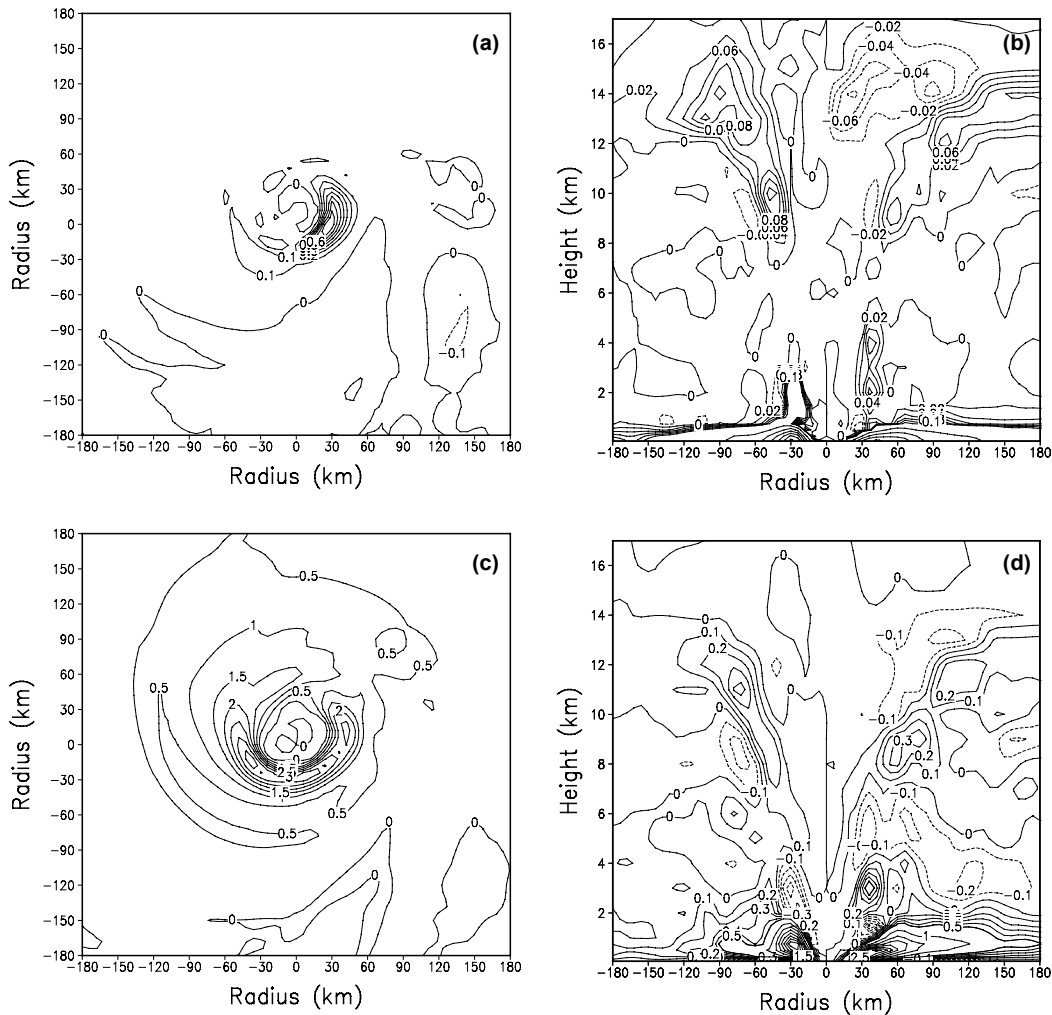


**Fig. 3.** Radial and tangential components in cylindrical coordinates by formula (1''). (a)  $h_r$  at 1 km; (b) the same as Fig. 1d but for  $h_t$ ; (c)  $h_t$  at 1 km. (d) the same as Fig. 1d but for  $h_t$ .

It is the sum of  $h_r$  with  $h_t$  (Eq. (1'')), the same as the sum of  $h_x$  with  $h_y$  (Eq. (1')). Figures 2c and 2d present the vertical component ( $h_z$ ). The scale of the horizontal components is 100 to 1000 times that of the vertical. This denotes that the horizontal components are the main parts of the helicity. The helicity in a hurricane mainly depends on its horizontal components. Both  $h_r$  and  $h_t$  are presented in Fig. 3. The values of the tangential component ( $h_t$ ) are larger than the radial component, just as the components of wind do.

Besides the values of the helicity, its inhomogeneous feature also depends on the horizontal components, especially on the tangential component. The patterns of Figs. 1d, 2b, and 3d are very alike.

The values of helicity at other integral times are also calculated. The results are similar and not presented here.

We are puzzled by the results. In hurricane An-

drew, the horizontal wind is no more than 50 times of the vertical velocity (Liu et al., 1999). How can the horizontal components of helicity be 100 to 1000 times the vertical one? The horizontal motion in a hurricane is cyclostrophic convergence from low level to middle level and cyclostrophic divergence from middle level to high level. How can the sign of helicity density be negative?

From Figs. 4 and 5 of the components of vorticity, our puzzle is solved completely. We can find from these figures that there are strong horizontal vortices in the hurricane. The horizontal vorticity is larger than the vertical except in the eye areas. Vortices at the boundary layer are dominated by the horizontal vorticity, whose order is ten times the vertical vorticity. In the layers above the planetary boundary layer, although the horizontal vorticity is smaller than that in the planetary boundary layer, it is still larger than

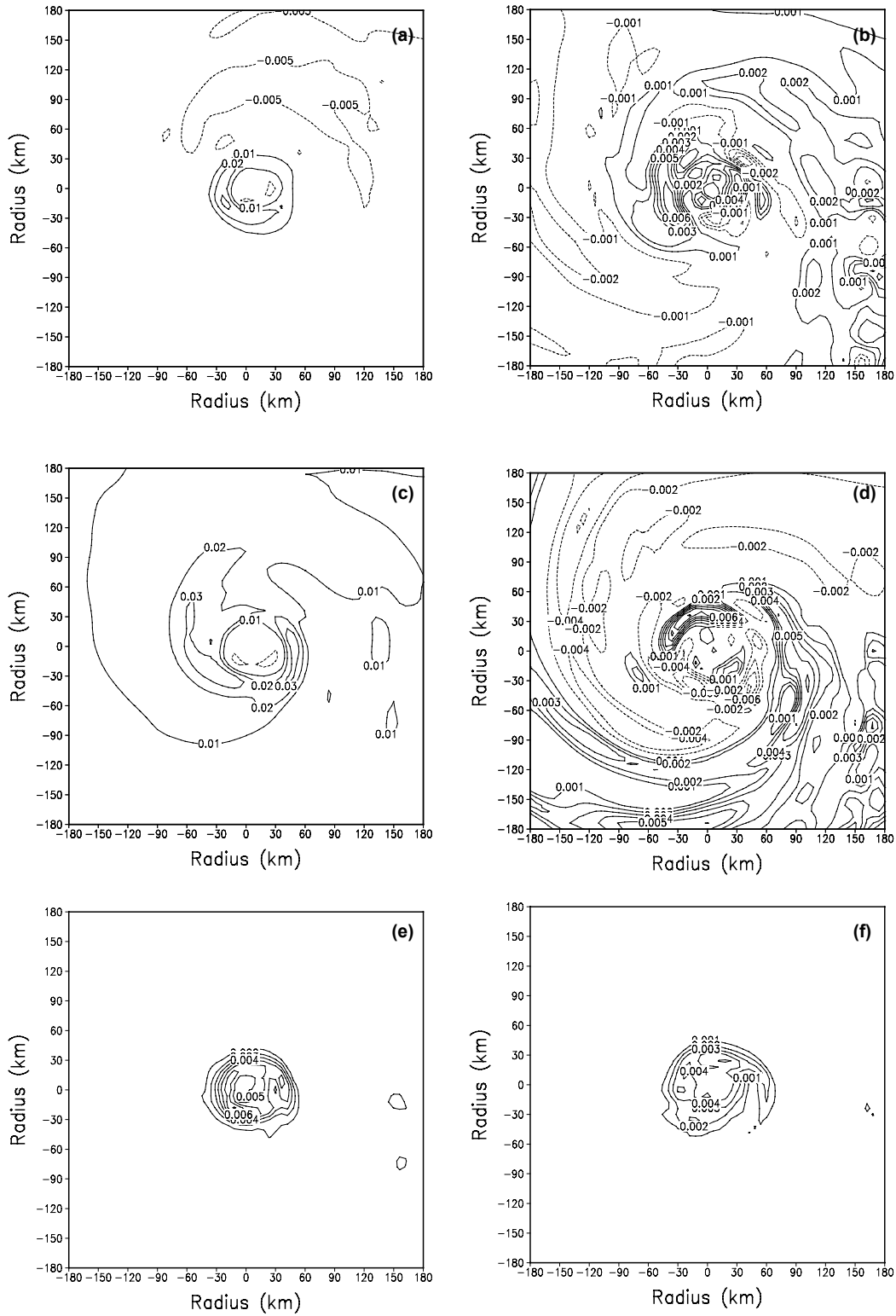


**Fig. 4.** Three components of vorticity ( $s^{-1}$ ) at 1 km (left panel) and 3 km (right panel). Contour interval is  $0.01 s^{-1}$  at (a) and (c) but  $0.001 s^{-1}$  at (b), (d), (e), and (f). (a) radial vorticity at 1 km; (b) the same as (a) but at 3 km; (c) tangential vorticity at 1 km; (d) the same as (c) but at 3 km; (e) vertical vorticity at 1 km; (f) the same as (e) but at 3 km.

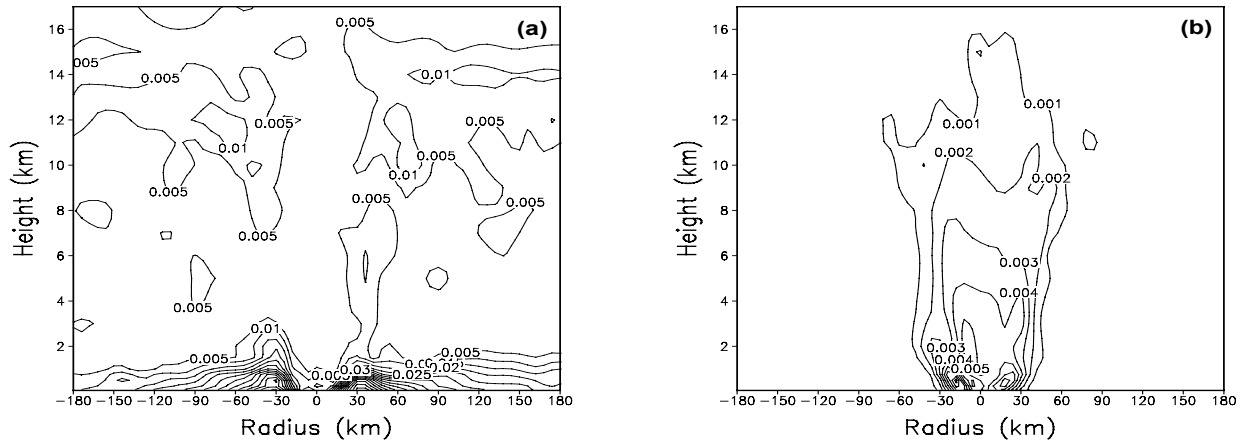


Fig. 5. Cross section of vorticity components along line AB in Fig. 1a. (a) horizontal vorticity; (b) vertical vorticity.

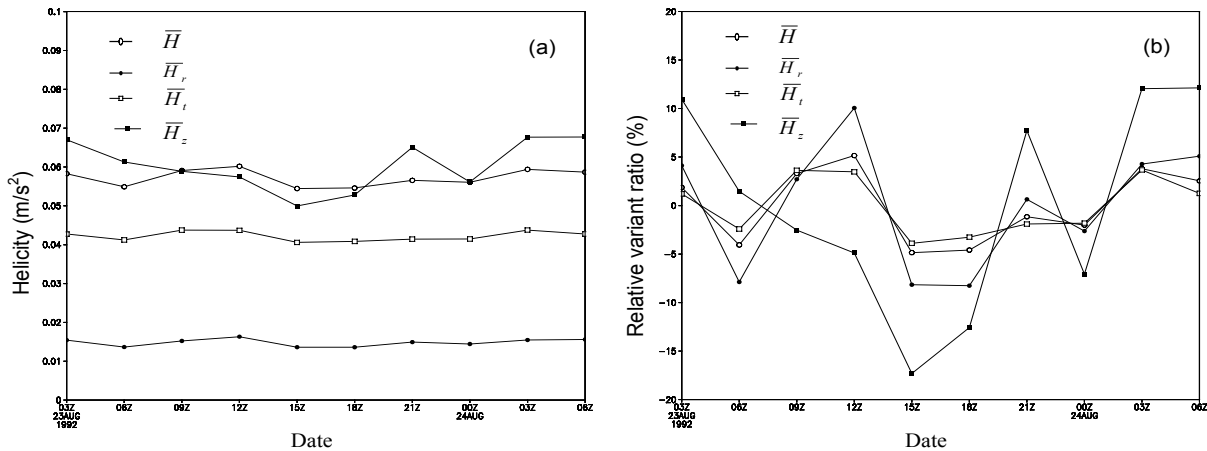


Fig. 6. Time variant curves of helicity (a) helicity of unit volume ( $\text{m s}^{-2}$ ) (the value of  $\bar{H}_z$  is multiplied by 500); (b) relative variant ratio (%).

the vertical vorticity. In the hurricane except in the inner eye, since the horizontal vorticity is larger than the vertical component, the vorticity vectors slant to the horizontal plane. The figures denote that the rotation around the horizontal axis is more significant than that around the vertical axis.

The figures also show that the horizontal vorticity is inhomogeneous (Figs. 4b and 4d). The variation of the horizontal vorticity is more significant than that of the vertical one. The vertical vorticity is always positive (Fig. 5b). The tangential and radial vorticities are positive in some places and negative in other places (Fig. 4d).

We can conclude that the helicity mainly depends on its horizontal component. The scale of the horizontal components of helicity is  $O(1 \text{ m s}^{-2})$  in the planetary boundary layer and  $O(0.1 \text{ m s}^{-2})$  in the layers above the boundary layer. It is only  $O(0.001 \text{ m s}^{-2})$  for the vertical component. The distribution

of helicity density is inhomogeneous and mainly determined by the horizontal components. The sign of helicity density can be negative in the eyewall and spiral rainband as well as in the inner eye.

The most important and interesting result is that there are strong horizontal vortices in the hurricane. The three-dimensional vortices slant to the horizontal plane except in the inner eye. The main vortical motion in the hurricane is found to be the horizontal vortex since the horizontal vorticity is larger than the vertical one.

#### 4. The conservation and horizontal inhomogeneous helical flows

In this section, the values of helicity and its source-sink terms at different integral times as well as the horizontal inhomogeneous helical flows are calculated.

We define  $\bar{H}$  as the total helicity of a unit volume.

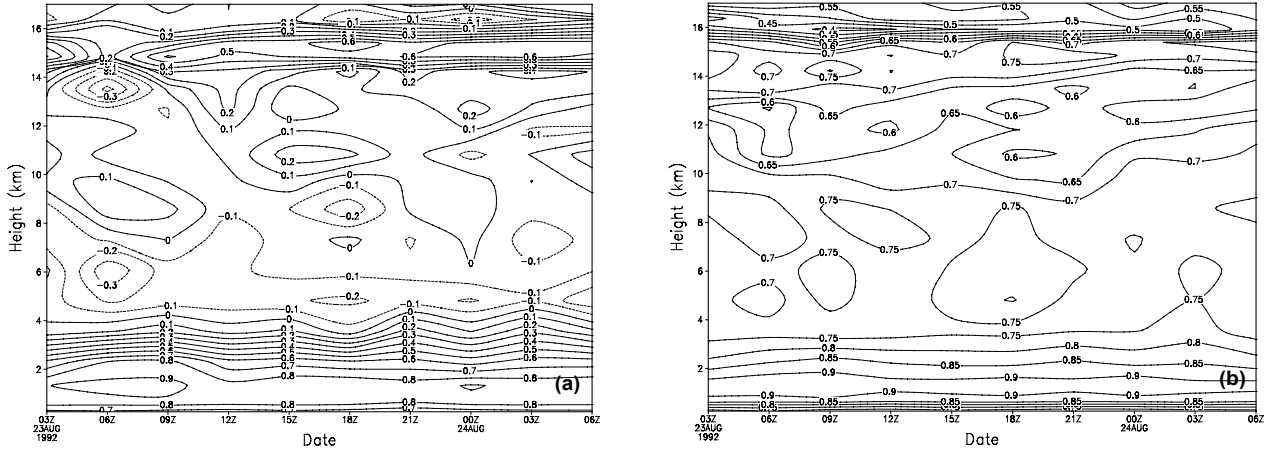


**Fig. 7.** Time-height section of layer-averaged relative helicity density. (a)  $\bar{r}_h$  (by formula (9)); (b)  $\bar{r}_{habs}$  (by formula (10)).

$$\bar{H} = \frac{\iiint (\mathbf{V} \cdot \nabla \times \mathbf{V}) d\tau}{\iiint d\tau} = \frac{H}{\iiint d\tau}.$$

We also define

$$\bar{H}_r = \frac{\iiint h_r d\tau}{\iiint d\tau},$$

$$\bar{H}_t = \frac{\iiint h_t d\tau}{\iiint d\tau},$$

$$\bar{H}_z = \frac{\iiint h_z d\tau}{\iiint d\tau},$$

as the radial, tangential, and vertical components of the total helicity of a unit volume. The integral volume is in the layer between 0 km to 17 km over an area within a radius of 180 km around the core of the hurricane.

Figure 6 presents the variation of total helicity as Andrew deepened before its landing. Figure 6a shows the variation of  $\bar{H}$ ,  $\bar{H}_r$ ,  $\bar{H}_t$ , and  $\bar{H}_z$  with respect to time. Figure 6b shows their relative variant rate, which is defined as

$$\frac{A - \bar{A}}{\bar{A}} \times 100\%,$$

where  $\bar{A}$  is the time-averaged value of  $A$ , and  $A$  can be one of  $\bar{H}$ ,  $\bar{H}_r$ ,  $\bar{H}_t$ , or  $\bar{H}_z$ . As the vertical component of helicity is small, the value of  $\bar{H}_z$  is multiplied by 500 in Fig. 6a. From Fig. 6, we can find that the variation of  $\bar{H}$  is small and its variant rate is no more than 5%. This denotes that helicity is approximately conserved as the hurricane deepens. However, the variations of the three components of helicity are different and the tangential component ( $\bar{H}_t$ ) is even more con-

servative than  $\bar{H}$ . Although the variant rate of  $\bar{H}_z$  is about 15% sometimes, it does not affect the conservation of total helicity as its value is small. The terms on the right-hand side of Eq. (8) are also calculated. It is shown that the magnitude of both terms is small and their signs are different so that their sum closes to zero. This means the helicity is conservative (figure omitted). The conclusion is drawn that helicity is approximately conserved as the hurricane deepens.

When calculating helicity density ( $h$ ) at different integral times, it is found that its time variation is significant. How can total helicity ( $\bar{H}$ ), and its integral, be time invariant?

Relative helicity, which is defined as

$$r_h = \frac{\mathbf{V} \cdot \nabla \times \mathbf{V}}{|\mathbf{V}| \cdot |\nabla \times \mathbf{V}|},$$

helps us to solve the question. We define  $\bar{r}_h$  as the layer-averaged relative helicity and  $\bar{r}_{habs}$ , the same as  $\bar{r}_h$  but for the average of absolute value. The integral area is an area within a radius of 180 km around the core of the hurricane.

$$\bar{r}_h = \frac{\iint r_h ds}{\iint ds}, \quad (9)$$

$$\bar{r}_{habs} = \frac{\iint |r_h| ds}{\iint ds}. \quad (10)$$

Figures 7a and b show the calculated results of formulas (9) and (10). Both the values of  $\bar{r}_h$  and  $\bar{r}_{habs}$  in the planetary boundary layer are more than 0.8. This means that fluids in the planetary boundary layer organize themselves to a nearly Beltrami flow, which is the highest helical flow. Although  $\bar{r}_h$  is limited by  $-0.3$  to  $0.3$ ,  $\bar{r}_{habs}$  ranges between  $0.7$  to  $0.8$  in the layers

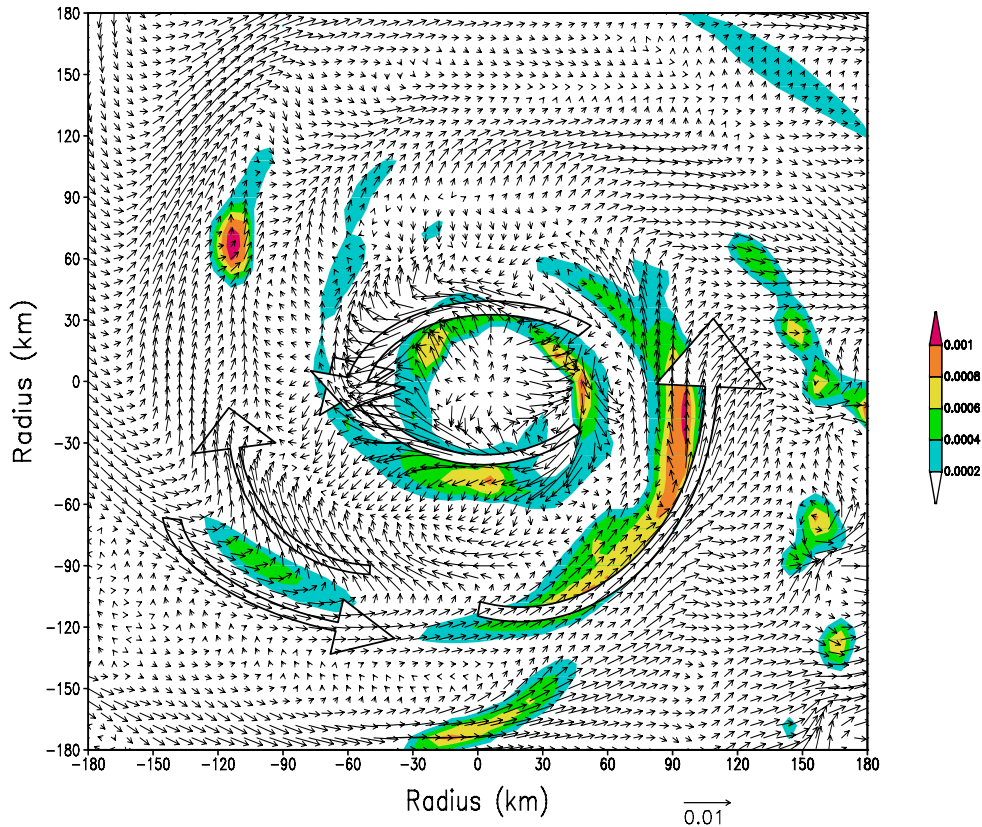


**Fig. 8.** Cloud water mixing ratio (shaded, more than  $0.0002 \text{ kg kg}^{-1}$ ) and horizontal vorticity vector (thin arrow,  $\text{s}^{-1}$ ) at 3 km. The white-thick arrows present the rotational axis of the main horizontal vortices.

above the boundary layer. It is shown that the flows in these layers are highly helical but relative helicity density is positive at some places and negative at other places. They counter each other when the volume integral is calculated. The flows in the layer above the boundary layer are highly helical too, but strongly inhomogeneous.

The conservation of helicity is used to explain the phenomena of strong horizontal vortices and inhomogeneous helical flows in the hurricane. As the horizontal component is the main part of helicity density and the flows in the hurricane are highly helical, total helicity  $H$  is approximately the integral of the scalar product of horizontal velocity with wind shear. When the hurricane deepens, horizontal velocity increases. The fluid must adjust wind shear to satisfy the conservation of  $H$ . We infer that strong wind shear and its significant variation are caused by the requirement of the conservation of helicity. Horizontal vortices and inhomogeneous helical flows are the results of conservation.

In this section, it is found that the helicity is conserved as the hurricane deepens. It is also found that there are horizontal inhomogeneous helical flows,

which are inferred to result from the fluids in the hurricane adjusting themselves to satisfy the conservation of total helicity.

### 5. The formation of the spiral rainband

After the characteristics of helicity are studied, it is interesting to investigate the relation of helicity with cloud and rain in a hurricane.

Brown (1980) and Eting (1985) stated that the formation of a cloud street is caused by the horizontal inhomogeneous helical secondary flow in the planetary boundary. As shown in sections 3 and 4, the horizontal inhomogeneous helical flow in the hurricane is also significant. This reminds us that the formation of the spiral rainband is similar to that of the cloud street.

The conjecture is supported by Fig. 8. In the figure, the regions with cloud water mixing ratio more than  $0.0002 \text{ kg kg}^{-1}$  are shaded. It is seen that all regions with high cloud water are on the left-hand side of the strong horizontal vortices and the areas with little or no cloud water are on the right-hand side of the vortex or region with weak horizontal vorticity. The case completely meets the ideal patterns of Brown (1980)

and Eting (1985), which have been used to explain the formation of the cloud street. Using the right hand rule, there is updraft caused or increased on the left-hand side of a strong horizontal vortex and downdraft on the right-hand side. The stronger and more inhomogeneous the horizontal vortex is, the more significant the vertical motion is. The nonlinear advection term and the slant term in the vorticity equation counteract each other in high helical flows. As the flows in a hurricane are highly helical, the horizontal vortices can be sustained due to the suppression of nonlinear interaction. The cloud and rain are caused or increased on the left-hand side of a strong horizontal vortex and reduced on the right-hand side. Cloud and rain are as inhomogeneous as the horizontal helical flow. The spiral rainband is closely related with the spiral horizontal helical flows.

Based on the results obtained so far, we can propose that the formation of the spiral rainband has a close correlation with the strong horizontal vortices and inhomogeneous helical flows, which are the results of the conservation of helicity. When the hurricane deepens, helicity is raised as velocity increases. Since the fluid must adjust itself to satisfy the conservation of helicity, horizontal strong vortices and inhomogeneous helical flows result. Updraft is caused or

increased on the left-hand side of a strong horizontal vortex and downdraft on the right-hand side (Fig. 9). The spiral rainband is closely related with inhomogeneous helical flow in the hurricane.

## 6. Conclusions

In this paper, the characteristics of helicity are studied by calculating the MM5 model output of a successfully simulated hurricane in addition to theoretical analyzing. Since there are great similarities in structure and organization for different hurricanes and typhoons, the characteristics shown in Figs. 1–8 can be considered as the general features of helicity in hurricanes and typhoons.

Helicity in a hurricane mainly depends on its horizontal component, whose magnitude is 100 to 1000 times larger than the vertical component. The scale of the horizontal component is  $O(1 \text{ m s}^{-2})$  in the planetary boundary and  $O(0.1 \text{ m s}^{-2})$  in the layers above the boundary layer. It is only  $O(0.001 \text{ m s}^{-2})$  for the vertical component.

Helicity is approximately conserved in a hurricane. Since the fluid has the intention to adjust the wind shear to satisfy the conservation of helicity as the hur-

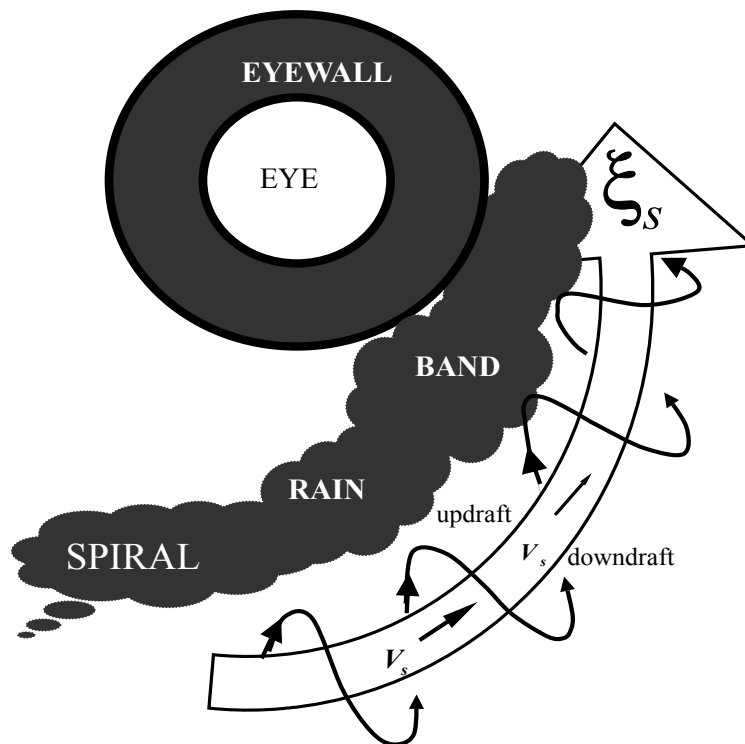


**Fig. 9.** Conceptual model of the formation of the spiral rainband. The black curve with arrows is the three-dimensional stream line around the horizontal rotational axis  $\xi_s$ .

ricane deepens, there appear significant horizontal vortices and inhomogeneous helical flows in the hurricane. The horizontal vorticity is larger than the vertical vorticity. The three-dimensional vortices slant to the horizontal plane except in the inner eye.

The formation of the spiral rainband is discussed by using the law of horizontal helical flows. It is closely related with the horizontal strong vortices and inhomogeneous helical flows.

**Acknowledgments.** The authors are grateful to Prof. Da-lin Zhang for supplying us with the MM5 model output of Andrew, and Prof. Tan Zhemin, Prof. Wang Yuan, Prof. Pan Yinong, and Dr. Fang Juan for their kind discussions, and an anonymous reviewer for his helpful comments. This research was sponsored by the National Natural Science Foundation of China under Grant No.40075011, 2001 PIA 20026 the National Key program for Developing Basic Sciences: CHeRES (G1998040907).

#### REFERENCES

- Brown, R. A., 1980: Longitudinal instabilities and secondary flows in the planetary boundary layer: A review. *Rev. Geophys. Space Phys.*, **18**, 683–697.
- Elsasser, W. M., 1956: Hydromagnetic dynamo theory. *Rev. Mod. Phys.*, **28**, 135–139.
- Eting, D., 1985: Some aspects of helicity in atmospheric flows. *Beitr. Phys. Atmos.*, **58**, 88–100.
- Lilly, D. K., 1986: The energy, energetics and propagation of rotating convection storms. Part II: Helicity and storm stabilization. *J. Atmos. Sci.*, **43**, 126–140.
- Lilly, D. K., 1990: Numerical prediction of thunderstorms—Has its time come? *Quart. J. Roy. Meteor. Soc.*, **116**, 779–798.
- Liu, Y., D.-L. Zhang, and M. K. Yau, 1997: A multiscale numerical study of Hurricane Andrew (1992). Part I: Explicit simulation and verification. *Mon. Wea. Rev.*, **125**, 3073–3093.
- Liu, Y., D.-L. Zhang, and M. K. Yau, 1999: A multiscale numerical study of Hurricane Andrew (1992). Part II: Kinematics and inner core structures. *Mon. Wea. Rev.*, **127**, 2597–2616.
- Maffatt, H. K., 1969: The degree of knottedness of tangled vortex lines. *J. Fluid Mech.*, **35**, 117–129.
- Maffatt, H. K., 1978: *Magnetic Field Generation in Electrically Conducting Fluids*. Cambridge University Press, 122pp.
- Maffatt, H. K., 1981: Some developments in the theory of turbulence. *J. Fluid Mech.*, **35**, 27–49.
- Tan Zhemin, and Wu Rongsheng, 1994: Helicity dynamics of atmospheric flow. *Advances in Atmospheric Sciences*, **11**, 175–188.
- Wu Rongsheng, and Tan Zhemin, 1989: Conservative laws on generalized vorticity and potential vorticity and its application. *Acta Meteor. Sinica*, **47**, 436–442.
- Wu Rongsheng, 2002: *Atmospheric Dynamics*. Higher Education Press, Beijing, 83–87.